



# Determining the Occurrence of a $3_{10}$ -Helix and an $\alpha$ -Helix in Two Different Segments of a Lipopeptaibol Antibiotic Using TOAC, a Nitroxide Spin-labeled $C^\alpha$ -Tetrasubstituted $\alpha$ -Aminoacid

Vania Monaco,<sup>a</sup> Fernando Formaggio,<sup>a</sup> Marco Crisma,<sup>a</sup> Claudio Toniolo,<sup>a,\*</sup>  
Paul Hanson,<sup>b</sup> Glenn Millhauser,<sup>b</sup> Clifford George,<sup>c</sup> Jeffrey R. Deschamps<sup>c</sup>  
and Judith L. Flippen-Anderson<sup>c</sup>

<sup>a</sup>Biopolymer Research Center, CNR, Department of Organic Chemistry, University of Padova, 35131 Padova, Italy

<sup>b</sup>Department of Chemistry and Biochemistry, University of California, Santa Cruz, CA 95064, USA

<sup>c</sup>Laboratory for the Structure of Matter, Naval Research Laboratory, Washington, DC 20375, USA

Received 13 April 1998; accepted 2 October 1998

**Abstract**—Trichogin GA IV is a 11-residue lipopeptaibol antibiotic exhibiting membrane modifying properties. We synthesized step-by-step by solution methods three trichogin analogues, each with a double Aib ( $\alpha$ -aminoisobutyric acid)→TOAC (2,2,6,6-tetramethylpiperidine-1-oxyl-4-amino-4-carboxylic acid) replacement. The strict similarity in the conformational propensities of Aib and TOAC allowed us to exploit these analogues in a detailed investigation of the conformation of this lipopeptaibol in different organic solvents and in a membrane-mimetic environment using in particular the double spin labeling ESR technique. We conclude that the secondary structure in solution remains essentially unchanged if compared to that previously found in the crystal state for trichogin. More specifically, the N-terminal region of the peptide folds in a  $3_{10}$ -helix, while the central and C-terminal regions are mainly  $\alpha$ -helical. An additional, significant proof for the modest plasticity of the trichogin structure was obtained by an X-ray diffraction analysis of the *n*Oct-[TOAC<sup>4,8</sup>, Leu-OMe<sup>11</sup>] analogue. For the three analogues permeability measurements revealed membrane-modifying properties comparable to those of natural trichogin. © 1999 Published by Elsevier Science Ltd. All rights reserved.

## Introduction

Beside the classical  $\alpha$ -helix and pleated  $\beta$ -sheet conformations the only other long-range structure that occurs significantly in polypeptide molecules is the  $3_{10}$ -helix. This structure was first proposed by Taylor<sup>1</sup> as early as 1941 and was later discussed in detail by Huggins,<sup>2</sup> Bragg et al.,<sup>3</sup> and Donohue.<sup>4</sup> As suggested by Bragg et al.,<sup>3</sup> polypeptide helices may be denoted by the symbol  $n_m$ , where  $n$  is the number of residues per turn and  $m$  the number of atoms contained in the ring closed by the intramolecular C=O...H-N hydrogen bond. Thus, the ideal  $\alpha$ -helix will be called  $3.6_{13}$ -helix. The  $3_{10}$ -helix (or, more properly, the  $3.0_{10}$ -helix) is more tightly wound than the  $\alpha$ -helix. The backbone torsion angles for the right-handed  $3_{10}$ -helix (approximately  $\phi = -57^\circ$ ,  $\psi = -30^\circ$ )<sup>5</sup> are within the same region of the

conformational map as those for the  $\alpha$ -helix (approximately  $\phi = -63^\circ$ ,  $\psi = -42^\circ$ ).<sup>6</sup> However, the intramolecular C=O...H-N hydrogen bonding schemes are different in the two helices, being of the 1←4 type (*trans*  $C_{10}$ -form or type-III  $\beta$ -bend<sup>7–9</sup>) in the  $3_{10}$ -helix, while of the 1←5 type (*trans, trans*  $C_{13}$ -form or  $\alpha$ -bend<sup>8,10,11</sup>) in the  $\alpha$ -helix. In this work we wish to describe the occurrence of a  $3_{10}$ -helical and an  $\alpha$ -helical segment within the same molecule, the lipopeptaibol antibiotic trichogin GA IV, both in solution and in the crystal state, despite the only slight differences in the parameters characterizing these two helices.

Peptaibols<sup>12</sup> are linear, Aib-rich peptides of fungal origin bearing at the C-terminus a 1,2-aminoalcohol. In general, these compounds exhibit membrane-modifying properties and, in particular, the long-sequence members of this family, such as alamethicin, are known to produce voltage-gated channels in planar membranes.<sup>13</sup> It is well established that these long helical peptaibols, which are able to span completely the membrane, self-aggregate according to a 'barrel-stave' mechanism.<sup>13</sup> Trichogin GA IV, isolated by Bodo and co-workers in 1992,<sup>14</sup> displays some special features with respect to the

**Key words:** Electron spin resonance;  $\alpha/3_{10}$ -helix; lipopeptaibol antibiotic; membrane-active peptides; X-ray diffraction.

\*Corresponding author at: Biopolymer Research Center, C.N.R., Department of Organic Chemistry, University of Padova, Via Marzolo, 1, 35131 Padova, Italy. Tel.: (39) (0)49-827-5247; fax: (39) (0)49-827-5239; e-mail: biop02@chor.unipd.it

other peptaibols. Its sequence contains only 11 residues (including the C-terminal aminoalcohol) and its N-terminal amino function is acylated by a long aliphatic (*n*-octanoyl) group. For this latter reason trichogin was classified as a lipopeptaibol. The primary structure of trichogin GA IV is as follows:



where *n*Oct stands for *n*-octanoyl, Aib for  $\alpha$ -aminoisobutyric acid, and Lol for leucinol. In spite of its limited main-chain length, trichogin GA IV does possess membrane-modifying properties, but its mechanism of action is not yet understood. In any case, it is clear that this lipopeptaibol is too short to fully span a biological membrane.

Our group has recently undertaken a systematic work aimed at examining the role of the N-terminal fatty acyl chain length on the membrane-modifying properties of trichogin GA IV.<sup>15</sup> Several  $\text{CH}_3(\text{CH}_2)_n\text{CO-[Leu-OMe}^{11}$ , where OMe is methoxy] trichogin analogues bearing at the N-terminus an acyl chain of variable length have been synthesized. We have demonstrated that a trichogin analogue should contain at least six carbon atoms in the acyl moiety in order to display a significant membrane activity. Furthermore, the [Leu-OMe<sup>11</sup>] trichogin analogue is as active as trichogin itself, suggesting that the C-terminal aminoalcohol does not play a major role in the membrane-modifying activity of the peptide. Trichogin GA IV adopts a helical conformation in the crystal state, as we have verified in an X-ray diffraction study.<sup>16</sup> It was shown that the peptide combines an incipient, distorted  $3_{10}$ -helix (residues 1–4) with a longer segment (residues 4–10) of slightly irregular  $\alpha$ -helix. The Aib<sup>4</sup> residue is found at the borderline between the two different types of helix. Moreover, the overall helical structure is amphipathic, with all hydrophobic groups (the *n*Oct group and Ile, Leu and Lol side chains) lying on the same face of the helix and the Gly residues on the

other face. The Aib methyl groups are aligned near the border between the two helical faces. Recently, in a solution study of the [Leu-OMe<sup>11</sup>] trichogin GA IV analogue using a combination of FTIR, CD and bidimensional NMR techniques, we have shown that this peptide is folded in a right handed, amphipathic, mixed  $3_{10}/\alpha$ -helical conformation in many organic solvents and in a sodium dodecylsulphate (SDS) micellar solution, the latter mimicking the membrane environment.<sup>17</sup> These conformational features differ only in some minor details from those found for trichogin GA IV in the crystal state.<sup>16</sup>

Electron spin resonance (ESR) has proven to be an excellent technique for studying peptide conformation in solution. ESR spectra of double spin labeled peptides are conformationally diagnostic and may allow to discriminate between  $3_{10}$ - and  $\alpha$ -helical conformations.<sup>18,19</sup> A direct relationship links helical geometry and distance between the two spin labeled residues, respectively placed in positions *i* and *j* along the peptide sequence (Fig. 1). If  $d(i,j)$  is the distance between side chains at position *i* and *j*, in an  $\alpha$ -helix the following rank is found:  $d(i,i+4) \leq d(i,i+3) < d(i,i+2)$ , while in a  $3_{10}$ -helix  $d(i,i+3) < d(i,i+4) < d(i,i+2)$ . The strength of spin–spin interaction between the spin labels in positions *i* and *j*, inferred from the ESR spectrum, accounts for their relative distance and consequently for the type of peptide helical structure in that region. In this area excellent results have recently been obtained by exploiting the paramagnetic aminoacid TOAC (2,2,6,6-tetramethylpiperidine-1-oxyl-4-amino-4-carboxylic acid).<sup>20–23</sup> TOAC<sup>23,24</sup> belongs to the family of C $\alpha$ -tetrasubstituted  $\alpha$ -aminoacids, the prototype of which is Aib (Fig. 2). In this aminoacid the spin labeled probe is severely conformationally restricted, as the nitroxyl nitrogen atom is incorporated in a cyclic moiety and rather close to the peptide backbone. Further studies have also demonstrated that TOAC, like Aib and the related 1-aminocyclohexane-1-carboxylic acid (Ac<sub>6</sub>C),<sup>25,26</sup> is a strong  $\beta$ -turn and  $3_{10}/\alpha$ -helical former.<sup>20–23,27</sup>

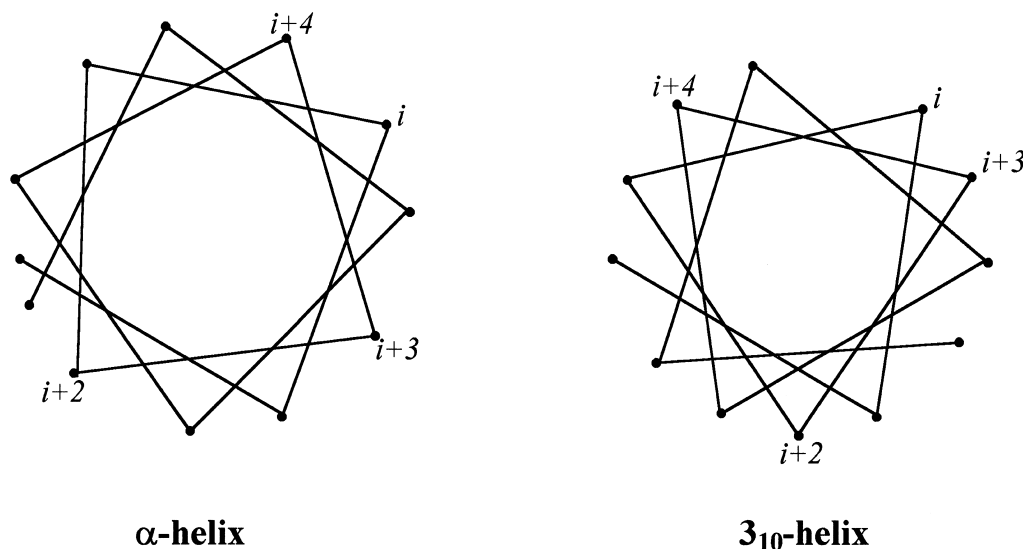
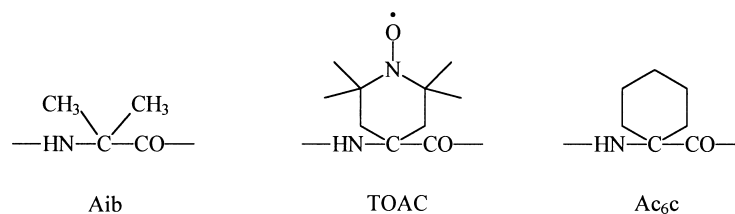


**Figure 1.** Helical wheels of a dodecapeptide in the  $\alpha$ -helical (left) and  $3_{10}$ -helical (right) conformations showing the distance relationship between the *i*, *i* + 2, *i* + 3, and *i* + 4 residues.

## Amino acids



## Peptides

## Abbreviation used

*n*Oct-TOAC-Gly-Leu-TOAC-Gly<sub>2</sub>-Leu-Aib-Gly-Ile-Leu-OMe  
*n*Oct-Aib-Gly-Leu-TOAC-Gly<sub>2</sub>-Leu-TOAC-Gly-Ile-Leu-OMe  
*n*Oct-TOAC-Gly-Leu-Aib-Gly<sub>2</sub>-Leu-TOAC-Gly-Ile-Leu-OMe

TOAC<sup>1,4</sup>  
 TOAC<sup>4,8</sup>  
 TOAC<sup>1,8</sup>

**Figure 2.** Structure of Aib, TOAC, the TOAC analogue 1-aminocyclohexane-1-carboxylic acid (Ac<sub>6</sub>c), and the trichogin analogues examined in this study.

To gather more information about the conformation adopted by [Leu-OMe<sup>11</sup>] trichogin GA IV in solution and in membrane-mimetic environment, we have decided to exploit the paramagnetic probe TOAC and the double spin labeling approach mentioned above. Therefore, we synthesized three analogues, each with a double Aib→TOAC replacement. The amino acid sequences are listed in Figure 2. The strong similarity in the structural propensities of Aib and TOAC allowed us to reasonably assume that the conformation of the three analogues might be close to that of the parent peptide. According to the crystal structure of trichogin,<sup>16</sup> the two labeled residues of the TOAC<sup>1,4</sup> analogue are placed in the positions *i* and *i* + 3, respectively, of the 3<sub>10</sub>-helical segment. In the TOAC<sup>4,8</sup> analogue, instead, the two TOAC residues are located in the positions *i* and *i* + 4 of the α-helical segment. In any case, in both analogues, if the conformation in solution is close to that found in the crystal state, a spin–spin interaction should be observed between the two spin labels. In TOAC<sup>1,8</sup> the two spin labeled residues are separated approximately by two turns of helix and are expected to be too far away from each other to interact. In this paper we describe the synthesis and characterization of the TOAC<sup>1,4</sup>, TOAC<sup>4,8</sup> and TOAC<sup>1,8</sup> trichogin GA IV analogues. We also report the results of our conformational studies of the three analogues using ESR and FTIR absorption in different solvents and in a membrane-mimetic environment and of the *n*-Oct-[TOAC<sup>4,8</sup>, Leu-OMe<sup>11</sup>] analogue in the crystal state using the X-ray diffraction technique. The membrane-modifying properties of these compounds are also described. A preliminary account of part of this work has already been presented.<sup>28</sup> A crystallographic study of the synthetic precursor [Fmoc<sup>0</sup>, TOAC<sup>4,8</sup>, Leu-OMe<sup>11</sup>] trichogin, (where Fmoc is 9-fluorenylmethyloxycarbonyl) has been reported.<sup>29</sup>

## Results and Discussion

## Peptide synthesis

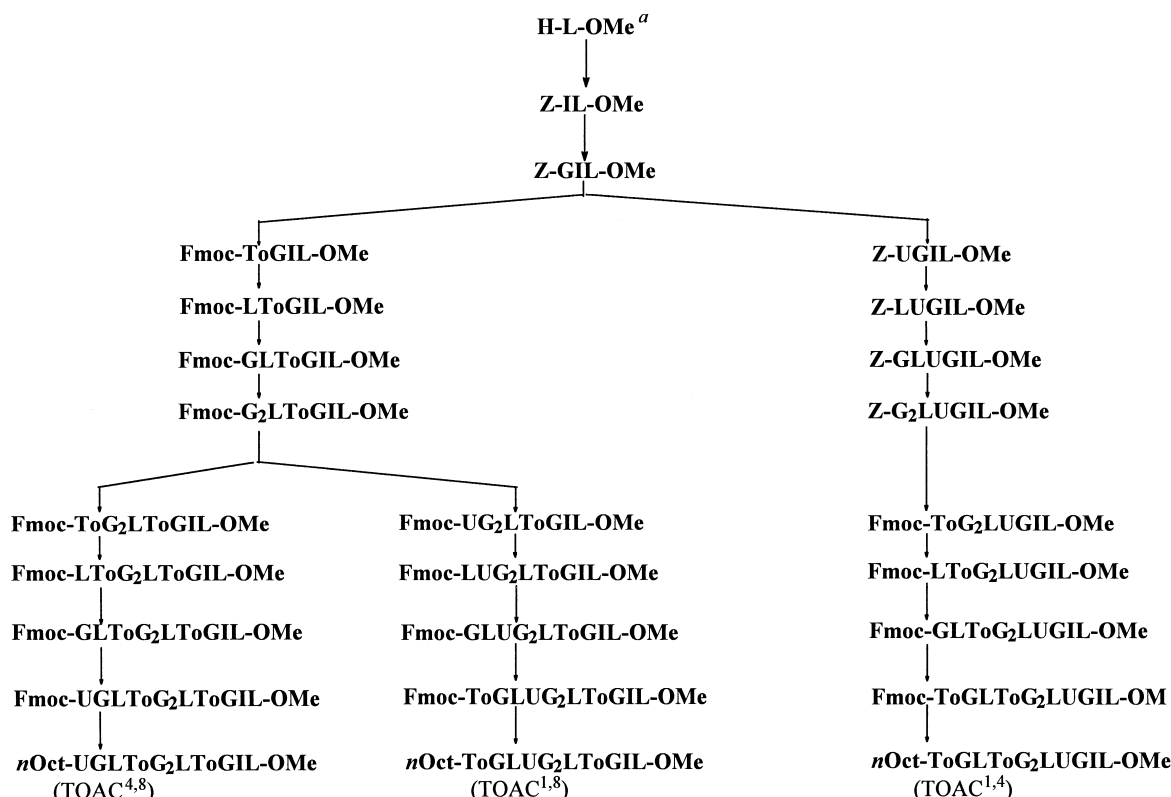
The free amino acid TOAC and its Fmoc *N*<sup>α</sup>-protected derivative were prepared according to published procedures.<sup>20</sup> The synthesis of the three TOAC-containing

trichogin GA IV analogues was performed step-by-step in solution, beginning from the C-terminal H-Leu-OMe residue, as described in Scheme 1. The synthesis and characterization of Z-Gly<sub>2</sub>-Leu-Aib-Gly-Ile-Leu-OMe (Z, benzyloxycarbonyl) and its short sequences were reported elsewhere.<sup>15</sup> As TOAC is unstable under the acidic and reducing conditions required to remove the classical Boc (*tert*-butoxycarbonyl) and Z groups, respectively, the Fmoc *N*<sup>α</sup>-protecting group was chosen for the elongation of TOAC-containing peptides.<sup>23</sup> The Fmoc group was removed by treatment with a 20% v/v diethylamine solution in CH<sub>2</sub>Cl<sub>2</sub>. The *N*-deprotected peptide was isolated via ‘flash chromatography’ on a silica gel column by eluting the dibenzofulvene side product with CH<sub>2</sub>Cl<sub>2</sub> and the desired peptide using a 8/2 CH<sub>2</sub>Cl<sub>2</sub>/MeOH (methanol) mixture. The Aib residues were incorporated using in situ formation of the symmetrical anhydride from Fmoc-Aib-OH. The same activation method was exploited for Leu-TOAC peptide bond formation, given the low reactivity of TOAC as a nucleophile.<sup>23</sup> The protein amino acids and the *n*Oct group were introduced by activating the carboxyl group with EDC/HOBt [EDC, *N*-ethyl-*N*′-(3-dimethylamino-propyl)carbodiimide; HOBt, 1-hydroxybenzotriazole]<sup>30</sup> and EDC/HOAt (HOAt, 1-hydroxy-7-aza-benzotriazole),<sup>31</sup> respectively.

The final compounds and intermediate sequences were obtained in a chromatographically homogeneous state and were characterized by polarimetry, TLC (thin-layer chromatography) in at least three different solvent systems, amino acid analysis, solid-state IR absorption and MALDI (matrix-assisted, laser-desorption ionization) mass spectrometry. The physical and analytical properties of the newly synthesized peptides are reported in Table 1.

## IR absorption

A preliminary conformational analysis of the TOAC<sup>1,4</sup>, TOAC<sup>4,8</sup>, and TOAC<sup>1,8</sup> trichogin analogues was carried out using FTIR absorption. This investigation was performed in CDCl<sub>3</sub> in the informative 3500–3200 cm<sup>−1</sup> and 1750–1600 cm<sup>−1</sup> regions (e.g., see Figure 3).<sup>32,33</sup> In the 3500–3200 cm<sup>−1</sup> region all spectra are characterized



**Scheme 1.** <sup>a</sup>One letter code for the amino acids. 'To' stands for TOAC and 'U' stands for Aib.

by a very strong absorption at  $3334\text{--}3326\text{ cm}^{-1}$  (N–H stretching band of H-bonded amide groups).<sup>33–35</sup> This band shows only a small concentration effect in the range  $10\text{--}0.1 \times 10^{-3}\text{ M}$ . Only at the  $0.1 \times 10^{-3}\text{ M}$  concentration one extremely weak band is seen in the  $3430\text{ cm}^{-1}$  region, which can be assigned to the N–H stretching mode of free (solvated) amide groups. The very high ratio between the intensities of the N–H stretching bands of H-bonded versus free amide groups strongly supports the view that these peptides are highly structured in this solvent of low polarity.<sup>35</sup> In the  $1750\text{--}1600\text{ cm}^{-1}$  region the position of the strong band at  $1664\text{--}1660\text{ cm}^{-1}$  (C=O stretching band of H-bonded amide groups) further supports this conclusion.<sup>36</sup> In this region an additional weak band is seen at  $1740\text{--}1735\text{ cm}^{-1}$  (ester C=O stretching band).

Globally, from our FTIR absorption analysis it is safe to conclude that in  $\text{CDCl}_3$  solution the three TOAC-based trichogin analogues adopt a helical conformation stabilized by intramolecular  $\text{C=O} \cdots \text{H-N}$  H-bonds. However, this analysis did not allow us to discriminate unambiguously between the types of helix ( $\alpha$ - versus  $3_{10}$ ) that are found, as, in particular, the potentially diagnostic position of the C=O stretching band differs only by less than  $5\text{ cm}^{-1}$  for these regular secondary structures.<sup>36</sup>

### Electron spin resonance

The ESR investigation was performed on the TOAC<sup>1,4</sup>, TOAC<sup>4,8</sup>, and TOAC<sup>1,8</sup> trichogin analogues in the three alcohols MeOH, EtOH (ethanol), HFIP (1,1,1,3,3,

3-hexafluoroisopropanol), and in ePC (egg phosphatidylcholine) liposomes. The line shapes of the spectra account for the spin–spin interaction between the two TOAC residues and consequently allow us to obtain valuable information on peptide conformation in that region.<sup>18–22</sup> Two mechanisms are responsible for the spin–spin interaction between two radicals: (a) the through-solvent  $J$ -coupling between the spins (scalar coupling), and (b) the electron–electron dipolar coupling (anisotropic coupling).<sup>37</sup> For rapidly tumbling molecules the dipolar coupling averages to zero and does not contribute to the spectrum (motionally-narrowed regime). The shape of the ESR spectrum is determined by the degree of  $J$ -coupling between the two radicals, the strength of which decreases exponentially with the distance  $d(i,j)$  between the labels, and by the isotropic hyperfine coupling  $a_n$  to the nitroxide nitrogen nucleus. A five-line spectrum with relative intensities 1:2:3:2:1 is expected in the case of strong coupling ( $J \gg a_n$ ). In the case of weak or no coupling ( $J \ll a_n$ ) the spectrum follows a three-line pattern (with relative intensities 1:1:1) as found for monoradical nitroxide-containing species. Between these two extreme cases the spectrum is characterized by broadened hyperfine lines which start to form complex multiplets as  $J$  increases with respect to  $a_n$ . It is appropriate to mention here that strong coupling may also derive from through-bond  $J$ -coupling.<sup>37</sup> This effect arises from spin polarization of the  $\sigma$ -bonds between the two nitroxides and it decreases exponentially with their number.<sup>38</sup> However, in our previous work on hexameric, TOAC-disubstituted peptides<sup>22</sup> we have verified that through-bond coupling contributes to the spectrum only if the spin labels are

**Table 1.** Physical and analytical properties for the TOAC-containing analogues of trichogin GA IV and their short sequences

Compound	Melting point (°C)	Crystalliz. solvent <sup>a</sup>	[α] <sub>D</sub> <sup>20</sup> (°) <sup>b</sup>	TLC			VIS	IR (cm <sup>-1</sup> ) <sup>d</sup>	Amino acid analysis	Mass spectrum
				R <sub>F1</sub>	R <sub>F2</sub>	R <sub>F3</sub>	R <sub>F4</sub>	λ <sub>max</sub> (e) <sup>c</sup>		
Fmoc-ToGIL-OMe <sup>g</sup>	169–171	AcOEt	–25.1 <sup>e</sup>	0.60	0.95	0.40	—	—	3323, 1730, 1690, 1651, 1532	G: 0.92, I: 1.02, L: 1.05, To: 1.02 M: 734, [(M+H) <sup>+</sup> ]: 736, [(M+Na) <sup>+</sup> ]: 759
Fmoc-LToGIL-OMe	166–168	AcOEt/EP	–54.7	0.75	0.95	0.45	—	—	3287, 1722, 1659, 1648, 1533	M: 847, [(M+H) <sup>+</sup> ]: 850, [(M+Na) <sup>+</sup> ]: 872
Fmoc-GLToGIL-OMe	145–147	AcOEt/EP	–71.7 <sup>f</sup>	0.70	0.95	0.40	—	—	3324, 1727, 1651, 1534	M: 904, [(M+H) <sup>+</sup> ]: 907, [(M+Na) <sup>+</sup> ]: 929
Fmoc-G <sub>2</sub> LToGIL-OMe	121–123	AcOEt/EP	–48.0	0.50	0.95	0.25	—	—	3332, 1732, 1656, 1536	M: 961, [(M+H) <sup>+</sup> ]: 963, [(M+Na) <sup>+</sup> ]: 985
Fmoc-ToG <sub>2</sub> LUGIL-OMe <sup>g</sup>	136–138	AcOEt/EP	–33.7	0.20	0.85	0.10	—	—	3332, 1731, 1659, 1535	M: 1046, [(M+H) <sup>+</sup> ]: 1048, [(M+Na) <sup>+</sup> ]: 1070, [(M+K) <sup>+</sup> ]: 1085
Fmoc-UG <sub>2</sub> LToGIL-OMe	199–201	AcOEt/EP	–43.7	0.35	0.90	0.10	0.85	—	3331, 1739, 1658, 1533	M: 1046, [(M+H) <sup>+</sup> ]: 1050, [(M+Na) <sup>+</sup> ]: 1071, [(M+K) <sup>+</sup> ]: 1086
Fmoc-ToG <sub>2</sub> LToGIL-OMe	152–154	AcOEt	–27.0	0.25	0.85	0.05	0.80	—	3342, 1735, 1659, 1534	M: 1158, [(M+H) <sup>+</sup> ]: 1163, [(M+Na) <sup>+</sup> ]: 1185
Fmoc-LToG <sub>2</sub> LUGIL-OMe	135–137	AcOEt/EP	–43.5	0.40	0.90	0.15	0.85	—	3321, 1727, 1660, 1534	M: 1159, [(M+H) <sup>+</sup> ]: 1164, [(M+Na) <sup>+</sup> ]: 1184
Fmoc-LUG <sub>2</sub> LToGIL-OMe	118–120	AcOEt/EP	–38.9	0.45	0.95	0.15	0.90	—	3324, 1727, 1662, 1534	M: 1159, [(M+Na) <sup>+</sup> ]: 1184, [(M+K) <sup>+</sup> ]: 1200
Fmoc-LToG <sub>2</sub> LToGIL-OMe	190–192	AcOEt/EP	–28.0	0.45	0.90	0.15	0.90	—	3330, 1727, 1662, 1530	M: 1271, [(M+H) <sup>+</sup> ]: 1275, [(M+Na) <sup>+</sup> ]: 1298, [(M+K) <sup>+</sup> ]: 1312
Fmoc-GLToG <sub>2</sub> LUGIL-OMe	138–140	AcOEt/EP	–31.6	0.20	0.90	0.05	0.80	—	3324, 1731, 1659, 1536	M: 1216, [(M+H) <sup>+</sup> ]: 1219, [(M+Na) <sup>+</sup> ]: 1242, [(M+K) <sup>+</sup> ]: 1259
Fmoc-GLUG <sub>2</sub> LToGIL-OMe	187–189	AcOEt	–23.9	0.25	0.95	0.05	0.85	—	3329, 1731, 1659, 1532	M: 1216, [(M+H) <sup>+</sup> ]: 1220, [(M+Na) <sup>+</sup> ]: 1242, [(M+K) <sup>+</sup> ]: 1257
Fmoc-GLToG <sub>2</sub> LToGIL-OMe	188–189	AcOEt	7.8	0.15	0.90	0.05	0.80	—	3337, 1731, 1664, 1532	M: 1328, [(M+Na) <sup>+</sup> ]: 1353, [(M+K) <sup>+</sup> ]: 1368
Fmoc-ToGLToG <sub>2</sub> LUGIL-OMe	160–162	AcOEt	2.9	0.05	0.80	—	0.65	—	3330, 1734, 1661, 1533	M: 1413, [(M+H) <sup>+</sup> ]: 1416, [(M+Na) <sup>+</sup> ]: 1438, [(M+K) <sup>+</sup> ]: 1454
Fmoc-ToGLUG <sub>2</sub> LToGIL-OMe	160–162	AcOEt/EP	–8.1	0.25	0.85	0.05	0.95	—	3332, 1734, 1659, 1532	M: 1413, [(M+Na) <sup>+</sup> ]: 1440, [(M+K) <sup>+</sup> ]: 1453
Fmoc-UGLToG <sub>2</sub> LToGIL-OMe	206–208	AcOEt/EP	19.3	0.10	0.80	—	0.95	—	3328, 1731, 1665, 1531	M: 1413, [(M+H) <sup>+</sup> ]: 1414, [(M+Na) <sup>+</sup> ]: 1436, [(M+K) <sup>+</sup> ]: 1452
<i>n</i> -Oct-ToGLToG <sub>2</sub> LUGIL-OMe	152–154	AcOEt	19.3	—	0.80	—	0.55	438 (12.8)	3329, 1741, 1661, 1536	M: 1317, [(M+H) <sup>+</sup> ]: 1319, [(M+Na) <sup>+</sup> ]: 1342, [(M+K) <sup>+</sup> ]: 1358
<i>n</i> -Oct-ToGLUG <sub>2</sub> LToGIL-OMe	185–187	AcOEt/EP	8.0	0.10	0.85	—	0.95	438 (14.0)	3325, 1744, 1661, 1537	M: 1317, [(M+H) <sup>+</sup> ]: 1321, [(M+Na) <sup>+</sup> ]: 1343
<i>n</i> -Oct-UGLToG <sub>2</sub> LToGIL-OMe	225–228	AcOEt	27.2	0.05	0.80	—	0.95	434 (17.6)	3329, 1745, 1663, 1538	M: 1317, [(M+H) <sup>+</sup> ]: 1321, [(M+Na) <sup>+</sup> ]: 1342

<sup>a</sup>AcOEt = ethyl acetate, EP = petroleum ether 60–80 °C.<sup>b</sup>c<sub>D</sub> = 0.5, MeOH.<sup>c</sup>λ<sub>max</sub> (nm) and ε (l × mol<sup>-1</sup> × cm<sup>-1</sup>); the VIS spectra were recorded in methanol.<sup>d</sup>The IR spectra were obtained in KBr pellets; only bands in the 3600–3200 and 1800–1500 cm<sup>-1</sup> regions are listed.<sup>e</sup>c<sub>D</sub> = 0.25, MeOH.<sup>f</sup>c<sub>D</sub> = 0.6, MeOH.<sup>g</sup>One letter code for the aminoacids; 'To' stands for TOAC and 'U' stands for Aib.

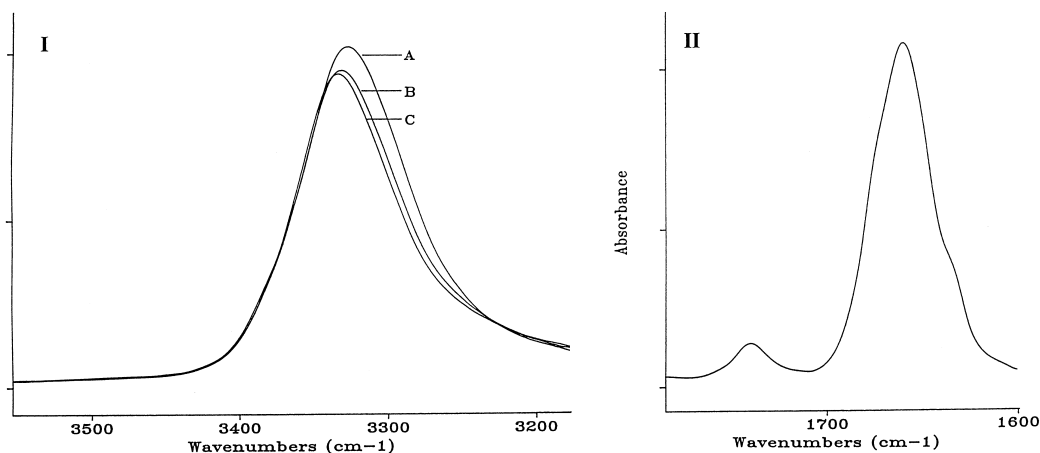


**Figure 3.** FTIR absorption spectra in the 3500–3200  $\text{cm}^{-1}$  region (I) and 1750–1600  $\text{cm}^{-1}$  region (II) of the TOAC<sup>4,8</sup> trichogin analogue in  $\text{CDCl}_3$  solution. In part (I) curves A, B, and C refer to  $1 \times 10^{-2}$  M,  $1 \times 10^{-3}$  M, and  $1 \times 10^{-4}$  M peptide concentrations, respectively.

adjacent in the peptide sequence. Since the peptides discussed in this article do not have adjacent spin labels, in the following discussion we shall simply refer to  $J$ -coupling as the through-solvent  $J$ -coupling.

The ESR spectra of the TOAC<sup>1,4</sup>, TOAC<sup>4,8</sup>, and TOAC<sup>1,8</sup> analogues in MeOH at 298 K are reported in Figure 4. At this temperature the peptides under examination are in the motionally-narrowed regime and the line shapes of the spectra are mainly determined by the through-space  $J$ -coupling mechanism. The spectrum of TOAC<sup>1,4</sup> is characterized by five lines, but the second and fourth lines are broadened. The spectrum of TOAC<sup>4,8</sup> displays three broadened lines, while in TOAC<sup>1,8</sup> the biradical interaction is nearly absent. These observations suggest that the rank order of the distances between the labels, which are inversely related to the strength of  $J$ -coupling, would be the following:  $d(1,4) < d(4,8) \ll d(1,8)$ . However, a possible modulation

of  $J$ , due to the fluctuations in the distance  $d(i,j)$ , can cause broadening of the second and fourth lines of the spectrum.<sup>39</sup> In the extreme case, a strong  $J$ -coupling can appear as a weak  $J$ -coupling.<sup>40</sup> For this reason the previous distance hierarchy needs to be verified by lowering the temperature.

Therefore, the spectra of TOAC<sup>1,4</sup>, TOAC<sup>4,8</sup>, and TOAC<sup>1,8</sup> in MeOH were also recorded at 200 K (Fig. 4). At this temperature the motionally-narrowed regime is no longer operative. In fact, the anisotropic contribution to the coupling (or electron–electron dipolar coupling), being not averaged to zero in slowly tumbling or immobilized systems (slow motion regime), dominates the spectrum of strongly interacting biradicals. Nevertheless, a distance ranking can be derived from the line width of the dipolar-broadened spectral component since the strength of dipolar coupling depends on  $1/d(i,j)^3$ .<sup>37</sup> The spectra of both TOAC<sup>1,4</sup> and TOAC<sup>4,8</sup>

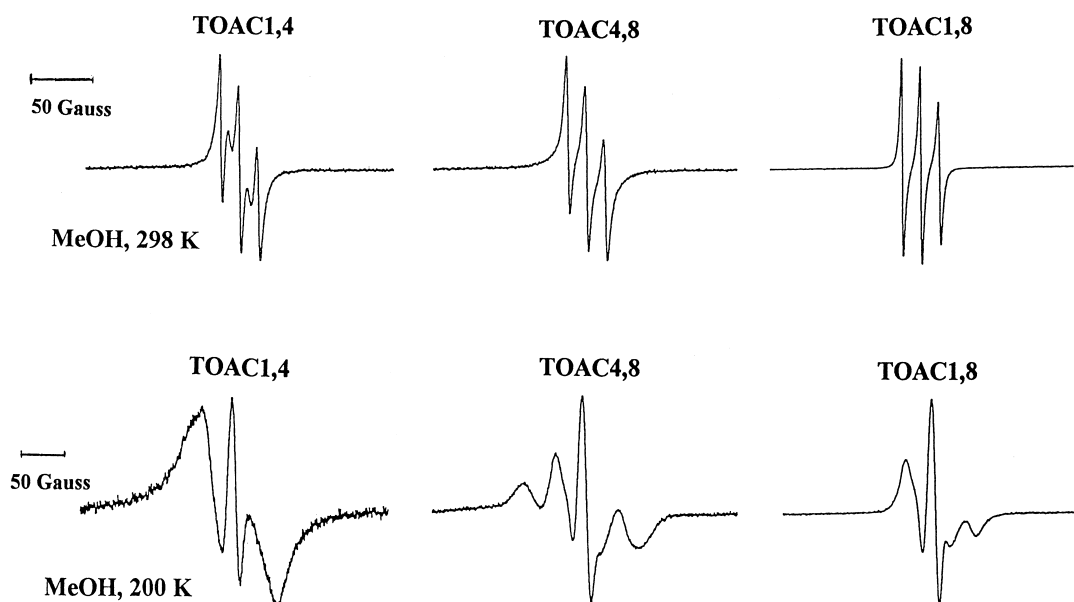


**Figure 4.** ESR spectra of the TOAC<sup>1,4</sup>, TOAC<sup>4,8</sup>, and TOAC<sup>1,8</sup> trichogin analogues at 298 K and 200 K in MeOH solution at  $1 \times 10^{-3}$  M peptide concentration. The spectra were recorded at 250 G scan width.

show a dipole-broadened component indicating a strong coupling between the labels. Although the spectrum of TOAC<sup>4,8</sup> would appear to result from an overlap of a strongly coupled spectrum with a weakly coupled spectrum, the splitting due to the dipolar interaction in TOAC<sup>4,8</sup> is larger than in TOAC<sup>1,4</sup>. In contrast, TOAC<sup>1,8</sup> shows no such splitting, thus indicating that in this compound the labels are too far from each other to interact. Then, the distance ranking given before needs to be modified as follows:  $d(4,8) < d(1,4) \ll d(1,8)$ . By means of molecular models it is possible to calculate the distances between the two labels in  $3_{10}$ - and  $\alpha$ -helices, respectively. The following  $\phi$ ,  $\psi$  values were used to build the models:  $-57^\circ$ ,  $-30^\circ$  for the  $3_{10}$ -helix, while  $-63^\circ$ ,  $-42^\circ$  for the  $\alpha$ -helix.<sup>6</sup> These distances are reported below:

	$3_{10}$ -helix	$\alpha$ -helix
TOAC <sup>1,4</sup>	6.43 Å	7.37 Å
TOAC <sup>4,8</sup>	9.96 Å	6.85 Å
TOAC <sup>1,8</sup>	13.98 Å	12.04 Å

The experimental data are consistent with either an  $\alpha$ -helical conformation in both regions or with an  $\alpha$ -helical conformation between residues 4 and 8 and a  $3_{10}$ -helical conformation between residues 1 and 4. The latter hypothesis seems to be favored if we compare our results with those previously obtained by our group on hexameric<sup>22</sup> and hexadecameric peptides.<sup>21</sup> In fact, the spectrum of TOAC<sup>1,4</sup> in MeOH at 200 K resembles that of the  $3_{10}$ -helical Hex 1,4 (Boc-TOAC-Ala<sub>2</sub>-TOAC-Ala<sub>2</sub>-OtBu, where OtBu is *tert*-butoxy) under the same experimental conditions. In an analogous way, the spectrum of TOAC<sup>4,8</sup> is reminiscent of that of the  $\alpha$ -helical 3KT-4,8 (Ac-Ala<sub>3</sub>-TOAC-Lys-Ala<sub>2</sub>-TOAC-Ala-Lys-Ala<sub>4</sub>-Lys-Ala-NH<sub>2</sub>, where Ac, acetyl). Altogether, these results are consistent with the X-ray diffraction structures of trichogin GA IV<sup>16</sup> and the [Fmoc<sup>0</sup>, TOAC<sup>4,8</sup>, Leu-OMe<sup>11</sup>] analogue.<sup>29</sup> In these two crystal-state structures the peptide conformation is essentially  $3_{10}$ -helical between residues 1–4 and  $\alpha$ -helical between residues 4–10. In the [Fmoc<sup>0</sup>, TOAC<sup>4,8</sup>, Leu-OMe<sup>11</sup>] analogue the distance between the two nitroxide groups is close to 6 Å.<sup>29</sup> This distance is somewhat shorter than that calculated above by using molecular models and crystallographically-determined  $\phi$ ,  $\psi$  values.<sup>6</sup> However, as pointed out above, the TOAC<sup>4,8</sup> spectrum acquired at 200 K in MeOH seems to originate from the overlapping of a spectrum with a weaker coupling to a spectrum with a stronger coupling. As a consequence, the peptide would mainly be  $\alpha$ -helical in the region between residues 4 and 8 but also flexible and flickering between the  $\alpha$ -helix and other energetically available conformations. Therefore, it is not surprising to find for this peptide in solution a distance between the two TOAC residues slightly different from that calculated.

A comparison of the spectra of the three TOAC doubly labeled analogues in MeOH at 298 K with those obtained at the same temperature in EtOH and HFIP (Fig. 5), gave us information on the role of solvent in affecting the peptide helical structure. The amount of

*J*-coupling in TOAC<sup>1,4</sup> and TOAC<sup>4,8</sup> tends to decrease on going from MeOH to EtOH. A higher flexibility of the helical structure and a shift in the equilibrium mixtures between helical and non-helical structures toward the latter might account for this result. In HFIP the spectra of both peptides show no *J*-coupling, indicating that in this highly polar solvent these compounds do not fold into an ordered conformation. Therefore, not surprisingly, the TOAC<sup>1,8</sup> spectra do not show any solvent dependence, as evidenced by the lack of *J*-coupling in all three alcohols.

The behavior of TOAC<sup>1,4</sup>, TOAC<sup>4,8</sup>, and TOAC<sup>1,8</sup> was also examined in 13 mM ePC liposomes (large unilamellar vesicles, LUV, 0.1  $\mu$ m diameter) at a temperature of 300 K (Fig. 6). The spectra of both TOAC<sup>1,4</sup> and TOAC<sup>4,8</sup> show a strong electron–electron dipolar coupling. This result indicates that the spin labels are immobilized, embedded in the lipid bilayer, and strongly interacting. Conversely, the spectrum of TOAC<sup>1,8</sup> is comparable to that of an immobilized monolabeled compound, suggesting no interaction between the two TOAC residues (as reported above for organic solvents). The sharp component in all of the spectra (dotted in Figure 6) probably arises from a small amount of monoradical impurity. The line width of the dipolar component is bigger for TOAC<sup>4,8</sup> than for TOAC<sup>1,4</sup>, as mentioned above for the MeOH solution at 200 K. This finding suggests that no dramatic conformational change takes place in the presence of the lipid bilayer. However, in the latter case the spectrum of TOAC<sup>4,8</sup> does not look like a superposition of two spectra, but rather it is reminiscent of that of a pure  $\alpha$  helix.

### X-ray diffraction

The X-ray diffraction structures of the two independent molecules **A** and **B** in the asymmetric unit of the TOAC<sup>4,8</sup> trichogin analogue are illustrated in Figure 7. Relevant backbone and side-chain torsion angles are given in Table 2. In Table 3 the intra- and inter-molecular H-bond parameters are listed.

As far as the geometrical features (bond lengths and bond angles; deposited) of the two TOAC residues are concerned, the N<sup>δ</sup>–O<sup>δ</sup> bond lengths of the two nitroxide groups [1.264(10) Å and 1.287(9) Å for molecule **A**, while 1.294(10) Å and 1.281(12) Å for molecule **B**], the external O<sup>δ</sup>–N<sup>δ</sup>–C<sup>γ</sup> bond angles [in the range 116.4(10)–120.2(8)°], and the internal bond angle at the N<sup>δ</sup> atom [121.3(7)° and 123.7(6)° for molecule **A**, while 123.2(7)° and 124.6(9)° for molecule **B**] compare well with those published for TOAC residues and related nitroxide-containing compounds.<sup>20,27,29</sup>

Predominantly helical molecules with right-handed screw sense are observed for both forms **A** and **B**. The general backbone conformational features of **A** and **B** differ only in few details. At the N-terminus of molecule **A** the carbonyl oxygen atom of the *n*Oct blocking group (O0A) is involved in a rather weak and somewhat distorted<sup>41–43</sup> 1 $\leftarrow$ 4 intramolecular H-bond with the peptide

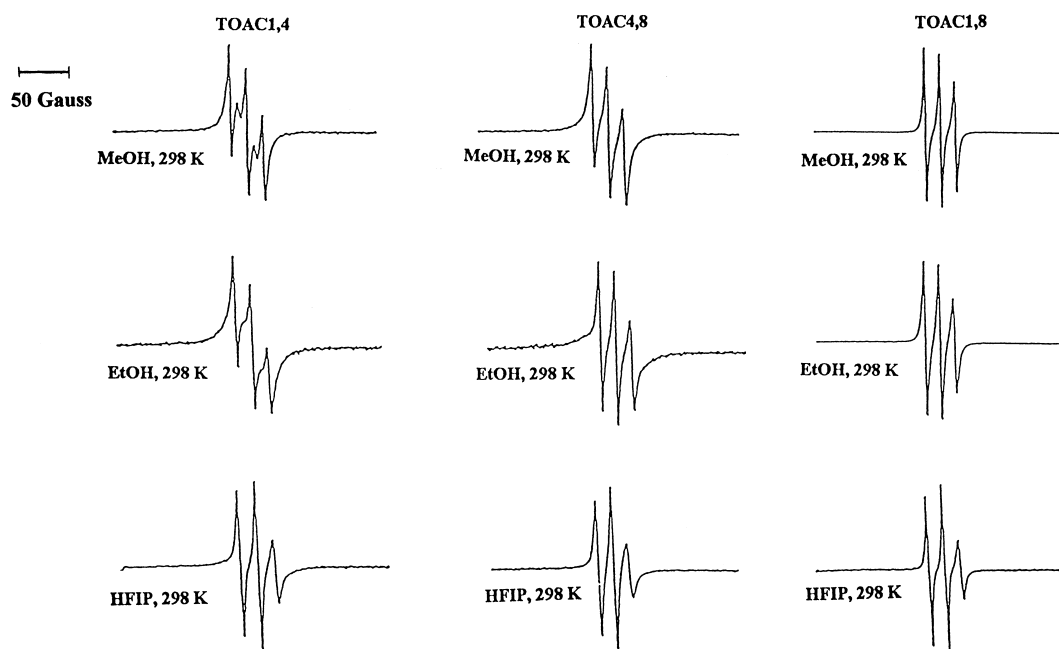


**Figure 5.** ESR spectra of the TOAC<sup>1,4</sup>, TOAC<sup>4,8</sup>, and TOAC<sup>1,8</sup> trichogin analogues at 298 K in MeOH, EtOH and HFIP ( $1 \times 10^{-3}$  M peptide concentration; 250 G scan width).

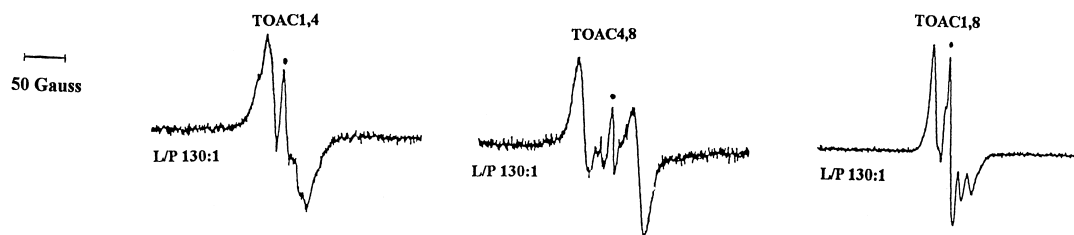


**Figure 6.** ESR spectra of the TOAC<sup>1,4</sup>, TOAC<sup>4,8</sup>, and TOAC<sup>1,8</sup> trichogin analogues at 300 K in 13 mM ePC LUV (pH 7.2;  $1 \times 10^{-3}$  M peptide concentration; scan width 350 G).

nitrogen (N3A) of Leu<sup>3</sup>. This C<sub>10</sub>-ring structure is characterized as a type-III  $\beta$ -turn.<sup>7–9</sup> However, the O0A atom is also the acceptor of a stronger H-bond from the peptide nitrogen (N4A) of TOAC<sup>4</sup> (double acceptor of intramolecular H-bonding<sup>44</sup>) giving rise to a C<sub>13</sub>-ring structure ( $\alpha$ -turn).<sup>8,10,11</sup> Therefore, the structure starts as a  $3_{10}/\alpha$ -helix, but then switches to a pure  $\alpha$ -helix, which leads the peptide nitrogen of Gly<sup>5</sup> (N5A) in a sufficiently close position to form an intramolecular H-bond with O1A. The pure  $\alpha$ -helix consists of five consecutive  $\alpha$ -turns which include the H-bonds between Gly<sup>5</sup> (N5A) and Aib<sup>1</sup> (O1A), Gly<sup>6</sup> (N6A) and Gly<sup>2</sup> (O2A), Leu<sup>7</sup> (N7A) and Leu<sup>3</sup> (O3A), TOAC<sup>8</sup> (N8A) and TOAC<sup>4</sup> (O4A), and Gly<sup>9</sup> (N9A) and Gly<sup>5</sup> (O5A). The carbonyl O6A atom of Gly<sup>6</sup> is not involved in the intramolecular H-bonding scheme, as the distances with the peptide nitrogens N9A and N10A (of Gly<sup>9</sup> and Ile<sup>10</sup>, respectively) are beyond the range of H-bonding ( $> 3.3$  Å), even though the geometry is correct. This helix distortion alters the peptide folding into a type-III  $\beta$ -turn (Ile<sup>10</sup> N10A  $\rightarrow$  Leu<sup>7</sup> O7A) followed by a type-I  $\beta$ -turn (Leu<sup>11</sup> N11A  $\rightarrow$  TOAC<sup>8</sup> O8A). Again, at the C-terminus a weakly H-bonded  $\alpha$ -turn stabilizes the helical structure (Leu<sup>11</sup> N11A  $\rightarrow$  Leu<sup>7</sup> O7A), as the low value of the Gly<sup>9</sup>  $\psi$  torsion angle is more than compensated for by

the high value of the Ile<sup>10</sup>  $\phi$  torsion angle. Thus, the carbonyl O7A atom, as the O0A atom discussed above, is a double acceptor of intramolecular H-bonding. The C-terminal Leu<sup>11</sup> residue is *semi*-extended. Only the -CO-NH-  $\omega_0$  torsion angle deviates more than 10° from the *trans* planarity.

The backbone conformation of molecule **B** differs from molecule **A** only at the C-terminus. In molecule **B** this region is characterized by a three-center (bifurcated) H-bond,<sup>45</sup> involving the Ile<sup>10</sup> N10B atom as the donor and both O6B (Gly<sup>6</sup>) and O7B (Leu<sup>7</sup>) atoms as the acceptors. The helix terminates with a type-III  $\beta$ -turn encompassing the sequence -Gly<sup>9</sup>-Ile<sup>10</sup>. The Leu<sup>11</sup> residue is found in the 'bridge' region of the conformational space.<sup>46</sup> Five consecutive  $\alpha$ -turns well illustrate the pure  $\alpha$ -helical nature of molecule **B** from N5B (Gly<sup>5</sup>) to N9B (Gly<sup>9</sup>) and from O1B (Aib<sup>1</sup>) to O5B (Gly<sup>5</sup>).

The nitroxide group of the two TOAC residues, separated by slightly more than one complete turn of the  $\alpha$ -helix, are oriented roughly perpendicular to the helix axis. The angle between the two N–O groups is 39.0(6)° in molecule **A** and 32.6(8)° in molecule **B**. The distance between the mid-points of the two N–O is 6.878(9) Å in



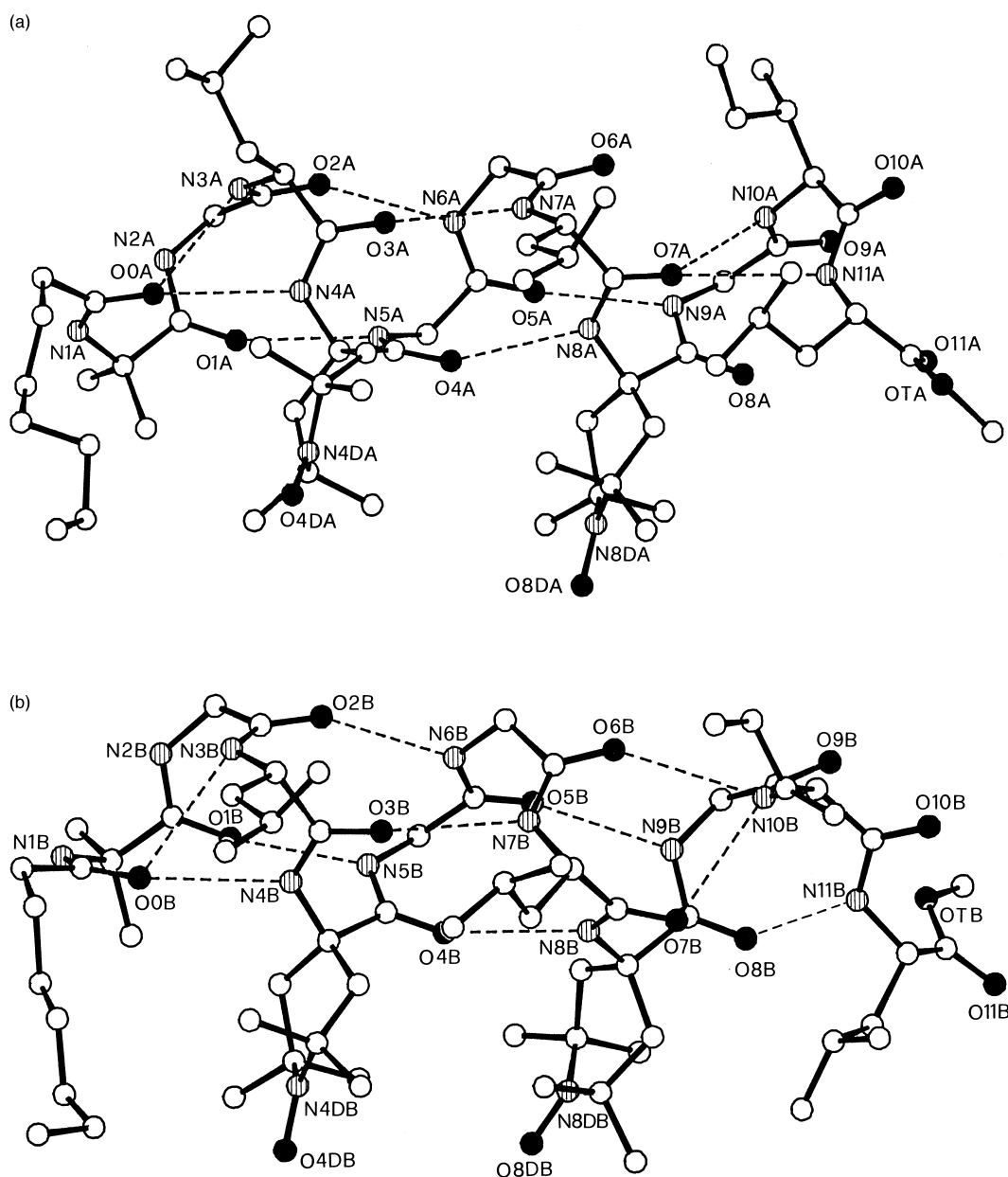


**Figure 7.** X-ray diffraction structures of the two crystallographically independent molecules **A** and **B** in the asymmetric unit of the TOAC<sup>4,8</sup> tri-chogin analogue with atom numbering. The intramolecular H-bonds are indicated by dashed lines.

molecule **A**, but only 5.989(10) Å in molecule **B**.<sup>20,27,29</sup> The hexa-atomic piperidiny rings are found in an approximate twist-boat conformation, with the following puckering parameters:<sup>47</sup>  $Q_T=0.664(9)$  Å,  $\Phi_2=89.7(7)^\circ$ ,  $\theta_2=91.5(7)^\circ$  for TOAC<sup>4</sup>, and  $Q_T=0.632(8)$  Å,  $\Phi_2=86.8(6)^\circ$ ,  $\theta_2=90.4(7)^\circ$  for TOAC<sup>8</sup> of molecule **A**;  $Q_T=0.637(10)$  Å,  $\Phi_2=90.2(8)^\circ$ ,  $\theta_2=89.5(8)^\circ$  for TOAC<sup>4</sup>, and  $Q_T=0.616(11)$  Å,  $\Phi_2=71.8(10)^\circ$ ,  $\theta_2=90.2(10)^\circ$  for TOAC<sup>8</sup> of molecule **B**. More precisely, the last conformation is intermediate between the twist-boat and the boat conformations. The angle between the normals to the average planes of the TOAC<sup>4</sup> and TOAC<sup>8</sup> ring systems is 12.2(2)° in molecule **A** and 6.1(3)° in molecule **B** (i.e., in each molecule the two TOAC residues are approximately parallel to each other). However, the angle between the N–O bonds is somewhat larger, 39.0(6)° in molecule **A** and 32.6(8)° in molecule **B**.

In addition to the backbone conformational difference at the C-terminus discussed above, molecules **A** and **B** show different side-chain torsion angles ( $\chi$ ).<sup>48</sup> In molecule **A** the Leu<sup>3</sup>, Leu<sup>7</sup>, and Leu<sup>11</sup> residues are found in conformations  $g^- (t g^-)$ ,  $t (g^+ t)$ , and  $g^- (t g^-)$ , respectively, while in molecule **B** the corresponding observed conformers are  $t (g^+ t)$ ,  $g^- (t g^-)$ , and  $g^- (t g^-)$ . The Ile<sup>10</sup> conformer is the common ( $t g^-$ )<sup>48</sup> in molecule **A**, while this same side chain is disordered in molecule **B**.

In the crystal packing rows of molecule **A** are formed along the  $x$ -direction through H-bonds from the Aib<sup>1</sup> N–H group to the Ile<sup>10</sup> C=O group. The same motif (along the same direction) holds for molecules **B**. In addition, the Gly<sup>2</sup> N–H group of molecule **A** is H-bonded to the nitroxide oxygen atom of TOAC<sup>8</sup> of the same molecule, giving rise to a zig-zag motif (twofold screw

**Table 2.** Relevant torsion angles (°) with their esd's for the two independent molecules **A** and **B** in the asymmetric unit of the TOAC<sup>4,8</sup> trichogin analogue

Torsion angle	Mol. A	Mol. B	Torsion angle	Mol. A	Mol. B
$\omega_0$	−169.5(7)	−174.3(8)			
$\phi_1$	−53.5(10)	−50.6(11)			
$\psi_1$	−47.6(9)	−48.8(10)			
$\omega_1$	−174.5(7)	−172.6(8)			
$\phi_2$	−66.6(9)	−69.2(12)			
$\psi_2$	−33.3(10)	−39.5(12)			
$\omega_2$	175.1(6)	174.7(8)			
$\phi_3$	−70.0(9)	−59.5(11)	$\chi_3^1$	−66.3(11)	177.1(9)
$\psi_3$	−41.2(10)	−48.5(11)	$\chi_3^{2,1}$	−177.8(12)	−170.1(10)
$\omega_3$	176.1(7)	180.0(16)	$\chi_3^{2,2}$	−53.6(16)	63.3(13)
$\phi_4$	−55.6(9)	−55.5(10)			
$\psi_4$	−45.9(9)	−48.2(9)			
$\omega_4$	178.4(6)	−178.5(7)			
$\phi_5$	−63.8(9)	−62.1(9)			
$\psi_5$	−45.6(10)	−42.0(10)			
$\omega_5$	179.2(6)	179.0(7)			
$\phi_6$	−60.8(9)	−63.7(10)			
$\psi_6$	−42.4(9)	−39.1(10)			
$\omega_6$	177.6(6)	177.4(7)			
$\phi_7$	−65.4(9)	−71.6(9)	$\chi_7^1$	−175.2(6)	−74.9(10)
$\psi_7$	−43.8(8)	−39.9(10)	$\chi_7^{2,1}$	59.6(10)	169.6(10)
$\omega_7$	179.2(6)	174.8(7)	$\chi_7^{2,2}$	−175.9(7)	−72.4(14)
$\phi_8$	−50.8(9)	−51.9(10)			
$\psi_8$	−47.2(9)	−47.3(10)			
$\omega_8$	−173.2(7)	−173.1(8)			
$\phi_9$	−65.8(12)	−69.0(11)			
$\psi_9$	−24.0(13)	−24.5(13)			
$\omega_9$	−176.1(8)	177.1(9)			
$\phi_{10}$	−101.0(9)	−66.5(12)	$\chi_{10}^{1,1}$	70.5(8)	155.5(13) <sup>a</sup>
$\psi_{10}$	−6.4(11)	−26.9(12)	$\chi_{10}^{1,2}$	−58.8(9)	−77.8(18) <sup>a</sup>
$\omega_{10}$	179.2(7)	179.7(9)	$\chi_{10}^2$	170.1(10)	−147.0(8) <sup>a</sup>
$\phi_{11}$	−89.5(10)	−85.3(11)	$\chi_{11}^1$	−69.9(9)	−57.0(13)
$\psi_{11}$	173.4(7)	−4.5(13)	$\chi_{11}^{2,1}$	−50.8(11)	−58.2(16)
$\omega_{11}$	174.8(9)	175.0(11)	$\chi_{11}^{2,2}$	−176.3(7)	178.4(12)

<sup>a</sup>Major conformer (see Experimental).

axis) along the  $y$ -direction. Conversely, the Gly<sup>2</sup> N–H group of molecule **B** is H-bonded to the Gly<sup>9</sup> C=O group of molecule **A** along a diagonal. The O1S water molecule bridges molecules **A** and **B**, by accepting a H-bond from the Leu<sup>3</sup> N–H group of molecule **B** (same asymmetric unit) and by donating a H-bond to the Gly<sup>9</sup> C=O group of molecule **A** along the same diagonal as above. Finally, the O2S water molecule is H-bonded to the Gly<sup>9</sup> C=O group of molecule **B**.

### Membrane-modifying properties

The membrane-modifying properties of the TOAC<sup>1,4</sup>, TOAC<sup>4,8</sup>, and TOAC<sup>1,8</sup> trichogin analogues were examined in comparison to that of trichogin. The results of the experiments of induced leakage of carboxy-fluorescein (CF) entrapped in ePC/Ch (cholesterol) small unilamellar vesicles are illustrated in Figure 8. All three analogues show a high activity, similar to that of trichogin. These findings may be related to the parallelism in the conformational propensities of Aib and TOAC residues and to the resulting similar conformations adopted by trichogin and its TOAC-disubstituted analogues. However, it is also evident that the interaction between the lipopeptaibol and the artificial membrane is not severely disturbed by the different balance

of the hydrophilic/hydrophobic properties of TOAC compared to those of Aib.

### Conclusions

Taken together, the present results have demonstrated that the three TOAC-disubstituted trichogin analogues TOAC<sup>1,4</sup>, TOAC<sup>4,8</sup>, and TOAC<sup>1,8</sup> adopt in solution a mixed  $\alpha/3_{10}$  helical conformation. In particular, by exploiting the double spin labeling ESR technique we have been able to show that the conformation characterizing trichogin and its double TOAC labeled analogues (including one discussed in the present paper) in the crystal state is largely preserved in solvents of medium polarity and in a membrane-like environment. The absence of biradical interaction observed for all peptides in HFIP indicates that there is little helical structure in this highly polar solvent. Interestingly, all of the three analogues are as active as trichogin itself in inducing membrane permeability from liposomes. Therefore, the present work has confirmed that the strong helical-forming, C $^{\alpha}$ -tetrasubstituted amino acid TOAC can replace Aib in a peptide sequence without causing any significant change neither in conformation nor in biological activity.

### Experimental

#### Peptide synthesis and characterization

Melting points were determined using a Leitz (Wetzlar, Germany) model Laborlux 12 apparatus and are not corrected. Optical rotations were measured using a Perkin–Elmer (Norwalk, CT) model 241 polarimeter equipped with a Haake (Karlsruhe, Germany) model L thermostat. Thin-layer chromatography was performed on a E. Merck (Darmstadt, Germany) Kiesegel 60F<sub>254</sub> precoated plates using the following solvent systems: I (CHCl<sub>3</sub>/EtOH 9/1), II [1-BuOH (1-butanol)/HOAc (acetic acid)/H<sub>2</sub>O, 3/1/1], III (toluene/EtOH, 7/1), IV (CHCl<sub>3</sub>/MeOH, 8/2). The chromatograms were examined by UV fluorescence or developed by Cl<sub>2</sub>/starch/KI or ninhydrin chromatic reaction as appropriate. All compounds were obtained in a chromatographically homogeneous state. Amino acid analyses were performed on a C. Erba (Rodano, Milan, Italy) model 3A30 amino acid analyzer after hydrolysis with 6N HCl for 48 h at 110 °C. The Aib color yield with ninhydrin is about 20 times lower than those of protein amino acids. The TOAC residue is unstable under the acidic conditions required for hydrolysis of the -CONH-, -OCONH- and -COO- bonds. Nevertheless, a signal (with a retention time very close to that of His) is detected, whose area is proportional to the number of TOAC residues in the sequence. MALDI mass spectra were obtained in the positive or negative linear mode at 10, 15, 20, or 30 KeV acceleration voltage on a reflex-time-of-flight mass spectrometer (Bruker, Karlsruhe, Germany), using either 2,5-dihydroxybenzoic acid or  $\alpha$ -cyano-4-hydroxybenzoic acid (Fluka, Buchs, Switzerland) as a matrix. The UV–VIS spectra were obtained using a Perkin–Elmer

**Table 3.** Hydrogen bond parameters for the two independent molecules **A** and **B** in the asymmetric unit of the TOAC<sup>4,8</sup> trichogin analogue

Type	Donor D	Acceptor A	Distance (Å) D–A	Distance (Å) H–A	Angle (°) D–H···A	Symmetry operation
Intramolecular Mol. A	N3-H	O0	3.047(9)	2.50	122	x, y, z
	N4-H	O0	3.059(9)	2.21	172	x, y, z
	N5-H	O1	3.042(9)	2.21	164	x, y, z
	N6-H	O2	2.946(9)	2.12	160	x, y, z
	N7-H	O3	2.921(9)	2.07	171	x, y, z
	N8-H	O4	2.984(9)	2.15	162	x, y, z
	N9-H	O5	3.015(9)	2.22	153	x, y, z
	N10-H	O7	3.098(8)	2.35	145	x, y, z
	N11-H	O7	3.239(9)	2.62	130	x, y, z
	N3-H	O0	3.172(9)	2.74	112	x, y, z
	N4-H	O0	3.069(9)	2.21	178	x, y, z
Mol. B	N5-H	O1	2.900(9)	2.07	161	x, y, z
	N6-H	O2	2.809(9)	1.98	160	x, y, z
	N7-H	O3	2.974(9)	2.14	164	x, y, z
	N8-H	O4	2.918(9)	2.08	166	x, y, z
	N9-H	O5	2.981(9)	2.20	150	x, y, z
	N10-H	O6	3.177(9)	2.53	133	x, y, z
	N10-H	O7	3.147(10)	2.48	135	x, y, z
	N11-H	O8	3.216(11)	2.48	144	x, y, z
	N1A-H	O10A	2.956(9)	2.12	166	x-1, y, z
	N2A-H	O8DA	2.848(9)	2.12	143	1-x, 1/2+y, -2-z
	N1B-H	O10B	2.869(11)	2.02	169	x-1, y, z
Intermolecular	N2B-H	O9A	2.755(11)	2.04	140	x-1, y, 1+z
	N3B-H	O1S	2.975(15)	2.20	151	x, y, z
	O1S-H	O9A	3.048(16)	—	—	x-1, y, 1+z
	O2S-H	O9B	2.699(13)	—	—	x, y, z-1
Peptide-solvent						

model Lambda 5 spectrophotometer. A quartz cell (Hellma, Müllheim, Germany) of 10 mm path length was used.

### IR absorption

The solid-state IR absorption measurements were performed on a Perkin–Elmer model 580 B spectrophotometer equipped with a Perkin–Elmer model 3600 data station, using the KBr disk technique. The solution FTIR spectra were recorded on a Perkin–Elmer model 1720X FTIR spectrophotometer, nitrogen-flushed, equipped with a sample-shuttle device, at 2 cm<sup>-1</sup> nominal

resolution, averaging 100 scans. Solvent (baseline) spectra were obtained under the same conditions. Cells with path length of 0.1, 1.0 and 10.0 mm (with CaF<sub>2</sub> windows) were used. Spectrograde deuteriochloroform (99.8% *d*) was purchased from Fluka.

### Electron spin resonance

X-band continuous wave spectra were obtained using a Bruker ESP 380 spectrometer equipped with a TE<sub>102</sub> cavity. Samples, each containing 50 µL of peptide solution, were sealed in glass capillary tubes. The spectra measured in organic solvents were independent of concentration in the range 0.1 to 10 mM. The spectra measured in ePC LUV were independent of concentration in the range of [lipid]/[peptide] 60 to 260. Peptide concentration was kept 0.1 mM in all experiments. The modulation frequency was 100 kHz. The spectra in organic solvents were recorded using a 0.25 G modulation amplitude, a scan amplitude of 250 G, and a power of 275 µW. The spectra recorded in ePC LUV were performed using a 1.25 G modulation amplitude, a scan amplitude of 350 G, and a power of 85 mW. The ePC LUV used in ESR experiments were prepared according to the procedure described by Hope et al.<sup>49</sup> Typically, 4 ml of a 10 mg mL<sup>-1</sup> CHCl<sub>3</sub> solution of ePC were first dried under a nitrogen flux and then under vacuum for 60 min. The lipidic film was hydrated with 2 mL of 100 mM MOPS buffer at pH 7.2 by vortexing. After five cycles of ‘freeze and thaw’ the lipidic suspension was extruded 10 times through two membranes of polycarbonate (Nucleopore-Polycarbonate, pore diameter: 0.1 µm, Costar). ePC was purchased from Avanti

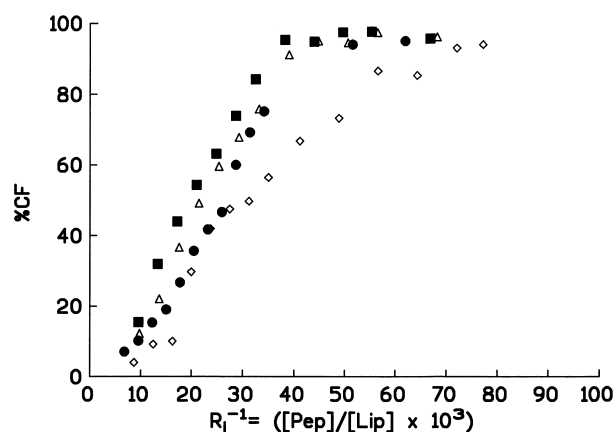


**Figure 8.** Peptide-induced CF leakage at 20 min for different ratios  $R_1^{-1} = [\text{peptide}]/[\text{lipid}]$  from ePC/Ch (7/3) small unilamellar vesicles: ■, TOAC<sup>1.4</sup>; ◇, TOAC<sup>4.8</sup>; △, TOAC<sup>1.8</sup>; ●, trichogin.

Polar-Lipids (Alabaster, AL), MOPS (3-[*N*-morpholino]-propanesulphonic acid) and HFIP from Sigma (St. Louis, MO), MeOH and EtOH from Fisher Scientific (Pittsburgh, PA).

### X-ray diffraction

Clear colorless crystals were grown from a MeOH/nitromethane solution by slow evaporation. Crystal data and refinement parameter information are given in Table 4. Diffraction data were collected on a computer controlled Bruker 1K Smart CCD system using a 5 kW Rigaku rotating anode source and Göbel mirrors. Unit cell dimensions were determined by a least-squares refinement of 360 centered reflections within  $-41 < 2\theta < 78^\circ$ . Data collection nominally covered a hemisphere in reciprocal space by combining six sets of exposures with different  $2\theta$  and  $\phi$  angles: each exposure covered a range of  $0.50^\circ$  in  $\omega$ . The crystal to detector distance was 5.05 cm. Data were collected to 0.9 Å resolution and a repetition of 50 of the initial frames at the end of the data set showed that the crystal remained stable during data collection. An empirical absorption correction was calculated with program SADABS<sup>50</sup> which uses equivalent reflections to calculate absorption effects. The structure was solved by the 'Shake and Bake' (SnB V1.5) direct-phasing program<sup>51</sup> using E values generated by XTAL V3.2.<sup>52</sup> One thousand trial structures were calculated and subjected to 95 cycles of iterative structure factor calculations, phase refinement, and density modification. Two of the trials, both with minimal function values<sup>53,54</sup> of 0.38, gave a solution for

the structure. The minimal function values for the incorrect structures ranged from 0.44 to 0.48. The structure was refined using the program SHELXL-97.<sup>55</sup> There were two peptide molecules (**A** and **B**), two water molecules, and two nitromethane molecules in the asymmetric unit. The 1779 parameters refined included coordinates and anisotropic thermal parameters for all non-H atoms. H-atoms were refined using a riding model. One of the two independent peptide molecules (**B**) had the Ile<sup>10</sup> side chain disordered over two sites, which were refined with 0.6 and 0.4 relative occupancies. One of the two water molecules (O1S) and both nitromethane molecules were disordered. Additional restraints were put on the distances, angles, and thermal parameters of the atoms in the two *n*-octanoyl chains to keep them chemically reasonable.

### Liposome leakage assay

Peptide-induced leakage from PC vesicles was measured at 20 °C using the CF-entrapped vesicle technique as previously described.<sup>56</sup> CF-encapsulated small unilamellar vesicles (ePC/Ch, 7/3) were prepared by sonication in Hepes (2-[4-(2-hydroxyethyl)-1-piperazinyl]ethanesulphonic acid) buffer, pH 7.5. The lipid concentration was kept constant ([egg PC + Ch] 0.6 mM), and increasing [peptide]/[lipid] molar ratios ( $R_i^{-1}$ ) were obtained by adding aliquots of MeOH solutions of peptides, keeping the final MeOH percent below 5% by volume. After rapid and vigorous stirring, the time course of the fluorescence change corresponding to CF escape was recorded at 520 nm (3 nm band pass) with  $\lambda_{exc}$  488 nm (3 nm band pass). The percentage of released CF at time  $t$  was determined as  $(F_t - F_0)/(F_T - F_0) \times 100$ , with  $F_0$  = fluorescence intensity of vesicles in the absence of peptide,  $F_t$  = fluorescence intensity at time  $t$  in the presence of peptide, and  $F_T$  = total fluorescence intensity determined by disrupting the vesicles by addition of 50  $\mu$ L of a 10% Triton (polyethylenglycol *tert*-octylphenyl ether) X-100 solution in water. The kinetics were stopped at 20 min. Fluorescence measurements were performed on a Perkin–Elmer model MPF-66 spectrofluorimeter in (1 cm  $\times$  1 cm) quartz cells (Hellma). ePC (type V-E, 100 mg mL<sup>-1</sup> solution in CHCl<sub>3</sub>/MeOH, 9/1) and cholesterol were purchased from Sigma, Hepes from Aldrich (St. Louis, MO), and Triton X-100 and CF from Fluka.

**Table 4.** Crystal data and structure refinement parameters for the TOAC<sup>4,8</sup> trichogin analogue

Empirical formula	C <sub>65</sub> H <sub>115</sub> N <sub>13</sub> O <sub>15</sub> ·H <sub>2</sub> O·CH <sub>3</sub> NO <sub>2</sub>
Formula weight (amu)	1397.8
Temperature	198(2) K
Wavelength	1.54178 Å
Crystal system	Monoclinic
Space group	P2 <sub>1</sub>
Unit cell dimensions	a = 20.384(1) Å $\alpha$ = 90° b = 19.142(2) Å $\beta$ = 106.73(1)° c = 21.200(1) Å $\gamma$ = 90°
Volume	7922.0(10) Å <sup>3</sup>
Z	4
Density (calculated)	1.17 Mg m <sup>-3</sup>
Absorption coefficient	0.70 mm <sup>-1</sup>
F(000)	3032
Crystal size	0.36 $\times$ 0.32 $\times$ 0.18 mm
$\theta$ range for data collection	2.26 to 58.92°
Index ranges	$-17 \leq h \leq 21$ , $-15 \leq k \leq 21$ , $-23 \leq l \leq 15$
Reflections collected	29424
Independent reflections	15176 [R(int) = 0.028]
Completeness to $\theta = 58.92^\circ$	84.4%
Absorption correction	Empirical
Refinement method	Full-matrix-block least-squares on F <sup>2</sup>
Data/restraints/parameters	15176/82/1779
Goodness-of-fit on F <sup>2</sup>	1.11
Final R indices [I > 2 $\sigma$ (I)]	R1 = 0.071, wR2 = 0.182
R indices (all data)	R1 = 0.088, wR2 = 0.199
Absolute structure parameter	0.0(3)
Extinction coefficient	0.00082(10)
Largest diff. peak and hole	0.58 and -0.37 e.Å <sup>-3</sup>

### References and Notes

1. Taylor, H. S. *Proc. Am. Phil. Soc.* **1941**, 85, 1.
2. Huggins, M. L. *Chem. Rev.* **1943**, 32, 195.
3. Bragg, L.; Kendrew, J. C.; Perutz, M. F. *Proc. Royal Soc. London* **1950**, A203, 321.
4. Donohue, J. *Proc. Natl. Acad. Sci. USA* **1953**, 39, 470.
5. IUPAC-IUB Commission on Biochemical Nomenclature, *Biochemistry* **1970**, 9, 3471.
6. Toniolo, C.; Benedetti, E. *Trends Biochem. Sci.* **1991**, 16, 350.
7. Venkatachalam, C. M. *Biopolymers* **1968**, 6, 1425.
8. Toniolo, C. C. R. C. *Crit. Rev. Biochem.* **1980**, 9, 1.
9. Rose, G. D.; Gierasch, L. M.; Smith, J. A. *Adv. Protein Chem.* **1985**, 37, 1.

10. Pavone, V.; Gaeta, G.; Lombardi, A.; Nastri, F.; Maglio, D.; Isernia, C.; Saviano, M. *Biopolymers* **1996**, *38*, 705.
11. Chou, K. C. *Biopolymers* **1997**, *42*, 837.
12. Benedetti, E.; Bavoso, A.; Di Blasio, B.; Pavone, V.; Pedone, C.; Toniolo, C.; Bonora, G. M. *Proc. Natl. Acad. Sci. USA* **1982**, *79*, 7951.
13. Sansom, M. S. P. *Prog. Biophys. Molec. Biol.* **1991**, *55*, 139.
14. Auvin-Guette, C.; Rebuffat, S.; Prigent, Y.; Bodo, B. *J. Am. Chem. Soc.* **1992**, *114*, 2170.
15. Toniolo, C.; Crisma, M.; Formaggio, F.; Peggion, C.; Monaco, V.; Goulard, C.; Rebuffat, S.; Bodo, B. *J. Am. Chem. Soc.* **1996**, *118*, 4952.
16. Toniolo, C.; Peggion, C.; Crisma, M.; Formaggio, F.; Shui, X.; Eggleston, D. S. *Nature: Struct. Biol.* **1994**, *1*, 908.
17. Monaco, V.; Locardi, E.; Formaggio, F.; Crisma, M.; Mammi, S.; Peggion, E.; Toniolo, C.; Rebuffat, S.; Bodo, B. *J. Pept. Res.* **1998**, *52*, 261.
18. Miick, S. M.; Martinez, G. V.; Fiori, W. R.; Todd, A. P.; Millhauser, G. L. *Nature (London)* **1992**, *359*, 653 (published corrections appeared in *Nature (London)* **1995**, *337*, 257).
19. Fiori, W. R.; Miick, S. M.; Millhauser, G. L. *Biochemistry* **1993**, *32*, 11957.
20. Toniolo, C.; Valente, E.; Formaggio, F.; Crisma, M.; Pilloni, G.; Corvaja, C.; Toffoletti, A.; Martinez, G. V.; Hanson, M. P.; Millhauser, G. L.; George, C.; Flippen-Anderson, J. L. *J. Pept. Sci.* **1995**, *1*, 45.
21. Hanson, P.; Martinez, G.; Millhauser, G.; Formaggio, F.; Crisma, M.; Toniolo, C.; Vita, C. *J. Am. Chem. Soc.* **1996**, *118*, 271.
22. Hanson, P.; Millhauser, G.; Formaggio, F.; Crisma, M.; Toniolo, C. *J. Am. Chem. Soc.* **1996**, *118*, 7618.
23. Toniolo, C.; Crisma, M.; Formaggio, F. *Biopolymers (Pept. Sci.)* **1998**, *47*, 153.
24. Marchetto, R.; Schreier, S.; Nakaie, C. R. *J. Am. Chem. Soc.* **1993**, *115*, 11042.
25. Karle, I. L.; Balaram, P. *Biochemistry* **1990**, *29*, 6747.
26. Toniolo, C.; Benedetti, E. *Macromolecules* **1991**, *24*, 4004.
27. Flippen-Anderson, J. L.; George, C.; Valle, G.; Valente, E.; Bianco, A.; Formaggio, F.; Crisma, M.; Toniolo, C. *Int. J. Pept. Protein Res.* **1996**, *47*, 231.
28. Monaco, V.; Toniolo, C.; Formaggio, F.; Crisma, M.; Hanson, P.; Millhauser, G. L.; George, C.; Flippen-Anderson, J. L.; Rebuffat, S.; Bodo, B. In *Proceedings of the 15th American Peptide Symposium*; Tam, J. P.; Kaumaya, P. T. P., Eds.; Kluwer: Dordrecht, 1998; in press.
29. Crisma, M.; Monaco, V.; Formaggio, F.; Toniolo, C.; George, C.; Flippen-Anderson, J. L. *Lett. Pept. Sci.* **1997**, *4*, 213.
30. König, W.; Geiger, R. *Chem. Ber.* **1970**, *103*, 788.
31. Carpino, L. A. *J. Am. Chem. Soc.* **1993**, *115*, 4397.
32. Bellamy, L. J. In *The Infra-Red Spectra of Complex Molecules*; Methuen: London, 1956.
33. Miyazawa, T. In *Poly- $\alpha$ -Amino Acids, Protein Models for Conformational Studies*; Fasman, G. D., Ed.; Dekker: New York, 1967; pp. 69–103.
34. Mizushima, S.; Shimanouchi, T.; Tsuboi, M.; Souda, R. *J. Am. Chem. Soc.* **1952**, *74*, 270.
35. Palumbo, M.; Da Rin, S.; Bonora, G. M.; Toniolo, C. *Makromol Chem.* **1976**, *177*, 1477.
36. Kennedy, D. F.; Crisma, M.; Toniolo, C.; Chapman, D. *Biochemistry* **1991**, *30*, 6541.
37. Luckhurst, G. R. In *Spin Labeling: Theory and Applications*, Berliner, L. J., Ed., Academic: New York, 1976; Vol. 1, pp 133–181.
38. Closs, G. L.; Forbes, M. D. E.; Piotrowiak, P. *J. Am. Chem. Soc.* **1992**, *114*, 3285.
39. Luckhurst, G. R. *Mol. Phys.* **1966**, *10*, 543.
40. Lemaire, H.; Rassat, A.; Rey, P.; Luckhurst, G. R. *Mol. Phys.* **1968**, *14*, 441.
41. Ramakrishnan, C.; Prasad, N. *Int. J. Protein Res.* **1971**, *3*, 209.
42. Taylor, R.; Kennard, O.; Versichel, W. *Acta Crystallogr.* **1984**, *B40*, 280.
43. Görbitz, C. M. *Acta Crystallogr.* **1989**, *B45*, 390.
44. Taylor, R.; Kennard, O. *Acc. Chem. Res.* **1984**, *17*, 320.
45. Taylor, R.; Kennard, O.; Versichel, W. *J. Am. Chem. Soc.* **1984**, *106*, 244.
46. Zimmerman, S. S.; Pottle, M. S.; Némethy, G.; Scheraga, H. A. *Macromolecules* **1977**, *10*, 1.
47. Cremer, D.; Pople, J. A. *J. Am. Chem. Soc.* **1975**, *97*, 1354.
48. Benedetti, E.; Morelli, G.; Némethy, G.; Scheraga, H. A. *Int. J. Pept. Protein Res.* **1983**, *22*, 1.
49. Hope, M. J.; Bally, M. B.; Webb, G.; Cullis, P. R. *Biochim. Biophys. Acta* **1985**, *812*, 55.
50. Sheldrick, G. M. *SADABS, Absorption Correction Program*, University of Göttingen, Germany, 1995.
51. Miller, R.; Gallo, S. M.; Khalak, H. G.; Weeks, C. M. *J. Appl. Crystallogr.* **1994**, *27*, 613.
52. Hall, S.; Subramanian, V. *GENEV Xtal 3.2 Reference Manual*; Hall, S. R.; Flack, H. D.; Stewart, J. M., Eds.; Universities of Western Australia, Geneva, and Maryland; Lamb: Perth, Australia, 1992.
53. Weeks, C. M.; DeTitta, G. T.; Miller, R.; Hauptman, H. A. *Acta Crystallogr.* **1993**, *D49*, 179.
54. Weeks, C. M.; De Titta, G. T.; Hauptman, H. A.; Thuman, P.; Miller, R. *Acta Crystallogr.* **1994**, *A50*, 210.
55. Sheldrick, G. M. *SHELXL. Program for Refinement of Crystal Structures*, University of Göttingen, Germany, 1997.
56. El Hajji, M.; Rebuffat, S.; Le Doan, T.; Klein, G.; Satre, M.; Bodo, B. *Biochim. Biophys. Acta* **1989**, *978*, 97.